

DISLOCATION-PRECIPITATE INTERACTION IN DISCRETE DISLOCATION DYNAMICS

PETR PAUŠ¹ AND MICHAL BENEŠ¹

Abstract. This contribution deals with the numerical simulation of dislocation dynamics by means of parametric mean curvature flow. Dislocations are described as an evolving family of closed and open smooth curves driven by the normal velocity. The equation is solved using direct approach by semi-discrete scheme based on finite difference method. Numerical stability is improved by tangential redistribution of curve points which allows long time computations and better accuracy. Our method contains an algorithm which allows topological changes. The results of the simulation of a dislocation and precipitate interaction are presented.

Key words. dislocation dynamics, topological changes, parametric approach

AMS subject classifications. 35K60, 35K65, 65N06, 68U10

1. Introduction. The dislocations are defined as irregularities or errors in crystal structure of the material. The presence of dislocations strongly influences many of material properties. Plastic deformation in crystalline solids is carried by dislocations. Theoretical description of dislocations is widely provided in literature such as [1–4]. Dislocation is a line defect of the crystalline lattice. Along the dislocation curve the regularity of the crystallographic arrangement of atoms is disturbed. The dislocation can be represented by a curve closed inside the crystal or by a curve ending on the surface of the crystal. At low homologous temperatures the dislocations can move only along crystallographic planes (gliding planes) with the highest density of atoms. The motion results in mutual slipping of neighboring parts of the crystal along the gliding planes.

This justifies the importance of developing suitable mathematical models [5–14]. From the mathematical point of view, the dislocations can be represented by smooth closed or open plane curves which evolve in time. Their motion is two-dimensional as they move in glide planes. The evolving curves can be mathematically described in several ways. One possibility is to use the *level-set method* [15–17], where the curve is defined by the zero level of some surface function. One can also use the *phase-field method* [18]. In our case, we use parametric approach [19, 20]

In this article, the interaction of precipitates and dislocation curves will be discussed and numerically simulated. The theory of such process was studied for example by Orowan [21] and Brown [22] and numerical simulation for example by Mohles [23, 24].

2. Dislocations and mean curvature flow. The interaction of dislocations and bulk elastic field can be approximately described using the curvature flow as follows (see [25]). We consider perfect dislocation curves with the Burgers vector $\vec{b} = (b, 0, 0)$ oriented in the x -direction of the x, y, z coordinate system. The dislocation curve motion Γ is located in a glide plane, in our case in the xz -plane. The glide of

¹Department of Mathematics, Faculty of Nuclear Sciences and Physical Engineering, Czech Technical University, Prague

dislocation is governed by the relaxation law in the form of the mean curvature flow equation in the direction of the normal vector

$$(2.1) \quad Bv = L\kappa + b(\tau_{app} + \tau_{pr}),$$

where B is a drag coefficient, and $v(x, t)$ is the normal velocity of a dislocation at $x \in \Gamma$ and time t . The term $L\kappa$ represents self-force expressed in the line tension approximation as the product of the line tension L and local curvature $\kappa(x, t)$. The term τ_{app} represents the local shear stress acting on the dislocation segment produced by the bulk elastic field. The term τ_{pr} stands for the stress generated by the precipitates. In our simulations, we consider “stress controlled regime” where the applied stress in the channel is kept uniform. This is an upper bound limit case. The other limiting case is “strain controlled regime” as described in [6, 7]. The applied stress τ_{app} is the same in every point of the line and for numerical computations we use $\tau_{app} = const.$

3. Parametric description. The motion law (2.1) in the case of dislocation dynamics is treated by parametrization where the planar curve $\Gamma(t)$ is described by a smooth time-dependent vector function $X : S \times I \rightarrow \mathbb{R}^2$, where $S = [0, 1]$ is a fixed interval for the curve parameter and $I = [0, T]$ is the time interval. The curve $\Gamma(t)$ is then given as the set

$$\Gamma(t) = \{X(u, t) = (X^1(u, t), X^2(u, t)), u \in S\}.$$

The evolution law (2.1) is transformed into the parametric form as follows. The unit tangential vector \vec{T} is defined as $\vec{T} = \partial_u X / |\partial_u X|$. The unit normal vector \vec{N} is perpendicular to the tangential vector and $\vec{N} \cdot \vec{T} = 0$ holds. The curvature κ is defined as

$$\kappa = \frac{\partial_u X^\perp}{|\partial_u X|} \cdot \frac{\partial_{uu} X}{|\partial_u X|^2} = \vec{N} \cdot \frac{\partial_{uu} X}{|\partial_u X|^2},$$

where X^\perp is a vector perpendicular to X with the same length. The normal velocity v is defined as the time derivative of X projected into the normal direction, $v = \partial_t X \cdot \partial_u X^\perp / |\partial_u X|$. The equation (2.1) can now be written as

$$B\partial_t X \cdot \frac{\partial_u X^\perp}{|\partial_u X|} = L \frac{\partial_{uu} X}{|\partial_u X|^2} \cdot \frac{\partial_u X^\perp}{|\partial_u X|} + b(\tau_{app} + \tau_{pr}),$$

which holds provided the vectorial evolution law is satisfied

$$(3.1) \quad B\partial_t X = L \frac{\partial_{uu} X}{|\partial_u X|^2} + b(\tau_{app} + \tau_{pr}) \frac{\partial_u X^\perp}{|\partial_u X|}.$$

This equation is accompanied by the periodic boundary conditions for closed curves, or by fixed-end boundary condition for open curves, and by the initial condition. These conditions are considered similarly as in [20].

The solution of (3.1) exhibits a natural redistribution property which is useful for short-time curve evolution [12, 26]. For long time computations with time and space variable force, the algorithm for curvature adjusted tangential velocity is used. This algorithm moves points along the curve according to the curvature, i.e., areas with higher curvature contain more points than areas with lower curvature. To incorporate a tangential redistribution, a tangential term α has to be added to the equation (3.1).

$$(3.2) \quad B\partial_t X = L \frac{\partial_{uu} X}{|\partial_u X|^2} + L\alpha \frac{\partial_u X}{|\partial_u X|} + b(\tau_{app} + \tau_{pr}) \frac{\partial_u X^\perp}{|\partial_u X|}.$$

This improves numerical stability and also accuracy of computation. Details are described in [8, 19].

4. Numerical scheme. For numerical approximation we consider a regularized form of (3.2) which reads as

$$(4.1) \quad B\partial_t X = L \frac{\partial_{uu} X}{Q(\partial_u X)^2} + L\alpha \frac{\partial_u X}{Q(\partial_u X)} + b(\tau_{app} + \tau_{pr}) \frac{\partial_u X^\perp}{Q(\partial_u X)},$$

where $Q(x_1, x_2) = \sqrt{x_1^2 + x_2^2 + \varepsilon^2}$ is a regularization term and ε a small parameter. The term ε serves as a regularization to avoid singularities when the curvature tends to infinity. We use the backward Euler semi-implicit scheme for numerical solution of the differential equation (3.2). The first derivative is discretized by backward difference as follows

$$\partial_u X|_{u=jh} \approx \left[\frac{X_j^1 - X_{j-1}^1}{h}, \frac{X_j^2 - X_{j-1}^2}{h} \right],$$

and the second derivative as

$$\partial_{uu} X|_{u=jh} \approx \left[\frac{X_{j+1}^1 - 2X_j^1 + X_{j-1}^1}{h^2}, \frac{X_{j+1}^2 - 2X_j^2 + X_{j-1}^2}{h^2} \right].$$

The approximation of the first derivative is denoted as $X_{\bar{u},j}$ and the second derivative as $X_{\bar{u}u,j}$.

The semi-implicit scheme for equation (4.1) has the following form

$$(4.2) \quad BX_j^{k+1} - Lt \frac{X_{\bar{u}u,j}^{k+1}}{Q^2(X_{\bar{u},j}^k)} - Lt\alpha_j \frac{X_{\bar{u},ej}^{k+1}}{Q(X_{\bar{u},j}^k)} = BX_j^k + tb(\tau_{app} + \tau_{pr}) \frac{X_{\bar{u},j}^{\perp k}}{Q(X_{\bar{u},j}^k)},$$

$$j = 1, \dots, m-1, k = 0, \dots, N_T - 1,$$

where $X_{\bar{u},j}^\perp$ is a vector perpendicular to $X_{\bar{u},j}$, and α_j is redistribution coefficient. $X_j^k \approx X(jh, kt)$, t is a time step and N_T is the number of time steps. The matrix of the system (4.2) for one component of X^{k+1} has the following tridiagonal structure:

$$\begin{pmatrix} B + \frac{2tL}{h^2 Q^2} - \frac{tL\alpha}{hQ} & \frac{-tL}{h^2 Q^2} & 0 & \dots \\ \frac{-tL}{h^2 Q^2} + \frac{tL\alpha}{hQ} & \ddots & \ddots & \ddots \\ 0 & \ddots & \ddots & \ddots \\ \vdots & \ddots & \ddots & \ddots \end{pmatrix}.$$

The scheme (4.2) is solved for each k by means of matrix factorization. Since there are two components of X , two linear systems are solved in each time step.

Since the direct (parametric) approach itself does not handle topological changes, an additional algorithm was incorporated which is described in detail in [13]. The algorithm is not supposed to be universal for every situation and possibility. Main purpose is to simulate topological changes that can happen during dislocation dynamics, i.e., topological changes such as merging or splitting of curves, closing of open curves, etc. The algorithm is designed for topological changes of curves which touch only in one point.

5. Simulation of precipitate and dislocation interaction. The hardening of materials caused by distributing precipitates or small particles of another phase is a well-known phenomenon and has been used to develop high-strength structural materials. There are several hardening methods, and all of them (except composites) are to make dislocation motion more difficult by introducing various obstacles. The obstacles are divided into several classes. Absolutely strong obstacles (dispersion hardening) completely block the movement of the dislocation and lead to so called Orowan mechanism [21–24]. Less strong obstacles (solid-solution hardening, precipitation hardening) slow down the movement of the dislocation by means of the attractive or repulsive interaction.

Our numerical simulations were performed under the following set of parameters:

| | |
|---------------------------|---|
| Burgers vector magnitude | $b = 0.25 \text{ nm}$ |
| Line tension | $L = 2 \text{ nN}$ |
| Drag coefficient | $B = 1.0 \cdot 10^{-5} \text{ Pa} \cdot \text{s}$ |
| Applied stress | $\tau_{app} = 40 \text{ MPa}$ |
| Weak precipitate stress | $\tau_{pr} = -10 \text{ MPa}$ |
| Strong precipitate stress | $\tau_{pr} = -50 \text{ MPa}$ |

The simulation of the Orowan mechanism (Orowan looping) is presented in the Fig. 5.1. Under the applied stress ($\tau_{app} = 40 \text{ MPa}$), the dislocation bows out between absolutely strong particles (Fig 5.1b). When the bowed-out dislocation becomes semi-circular in shape, it splits and leaves the Orowan loop around the obstacle (Fig 5.1c). The formation of the Orowan loops makes the dislocation motion more and more difficult and results in a material hardening. This mechanism will happen for every absolutely strong obstacle (Fig 5.1f) unless the obstacles are too close to each other. In that case, formation of Orowan islands happens.

If the obstacles are close to each other, the dislocation cannot go through them and, under the applied stress ($\tau_{app} = 40 \text{ MPa}$), it surrounds the whole cluster of obstacles and creates the Orowan island (Fig 5.2). There are 4 obstacles in the distance of approximately 90 nm. Under some higher applied stress, the island would disappear leaving only Orowan loops around the obstacles.

The simulation in Fig. 5.3 shows another configuration of the obstacle cluster. There are 9 obstacles with random positions. The formation of the Orowan island under applied stress ($\tau_{app} = 40 \text{ MPa}$) is better visible than in Fig. 5.2. Again, if the applied stress is increased, the island would disappear and only Orowan loops would remain.

The lowest obstacle (dashed line) in Fig. 5.3 is set up as a weak obstacle so it only slows the movement of the dislocation in the gliding plane. This is visible in Figs. 5.3a and 5.3b.

6. Conclusion. The simulation of dislocation dynamics is important in practice as dislocations affect many material properties. Our model based on parametric mean curvature flow is suitable for the simulation of real phenomena and we presented the application in material hardening, i.e. the formation of Orowan loops and Orowan islands by the gliding dislocation. The numerical simulation requires the redistribution of discretization points as the curve changes shape dramatically. The parametric approach itself cannot handle topological changes and we had to introduce the algorithm for such changes into the model.

Acknowledgments. This work was supported by the grant of the Ministry of Education of the Czech Republic MSM6840770010 "Applied Mathematics in Technical

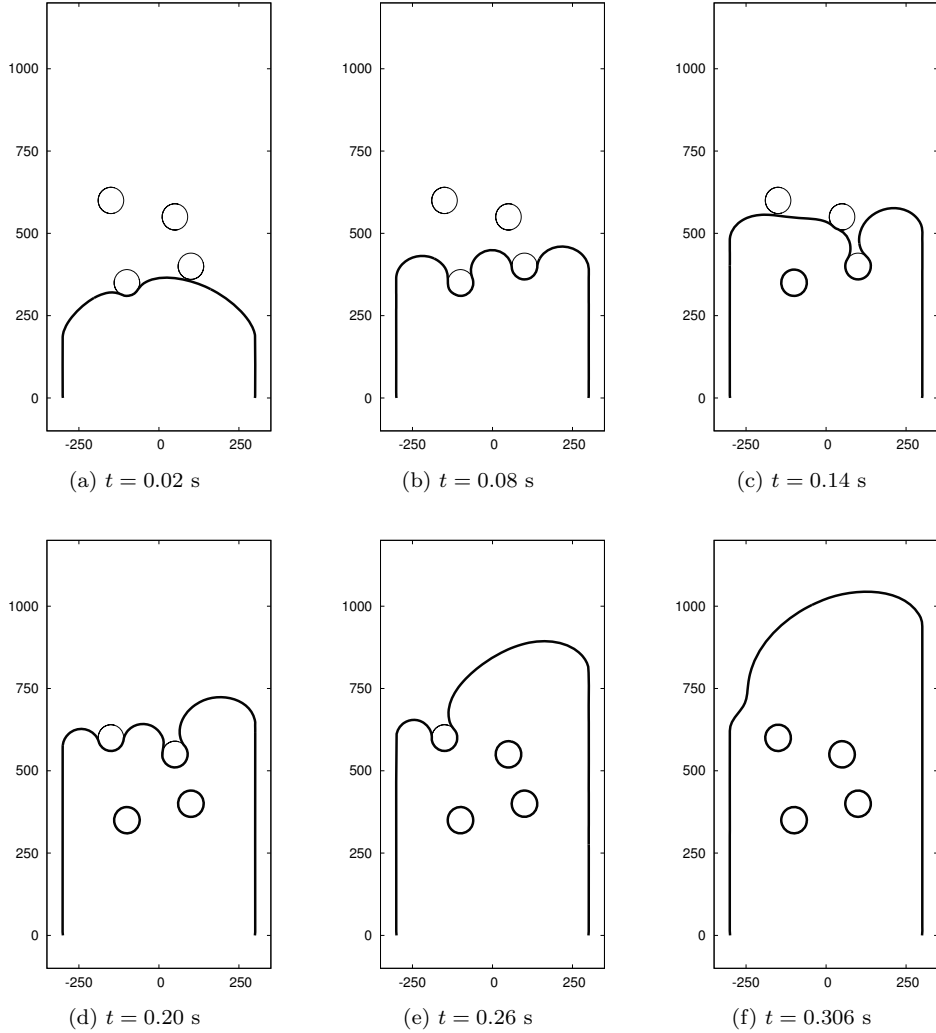


Fig. 5.1: Evolution through a cluster of obstacles and formation of the Orowan loops, $\tau_{app} = 40$ MPa, $t \in (0, 0.306)$, curve discretized by $M = 300$ nodes, dimensions in nm.

and Physical Sciences”, by the project ”Jindřich Nečas Center for Mathematical Modeling”, No. LC06052 of the Ministry of Education of the Czech Republic and by the project ”Two-Scale Discrete-Continuous Dislocation Dynamics” No. P108/12/1463 of the Grant Agency of the Czech Republic.

REFERENCES

- [1] J.P. HIRTH AND J. LOTHE. *Theory of Dislocations*. John Wiley, New York (1982).
- [2] F. KROUPA. *Long-range elastic field of semi-infinite dislocation dipole and of dislocation jog*. *Phys. Status Solidi* **9** (1965), 27–32.
- [3] F. KROUPA. *Dislocations in Solid State*. (in Czech) SNTL, Praha (1966).

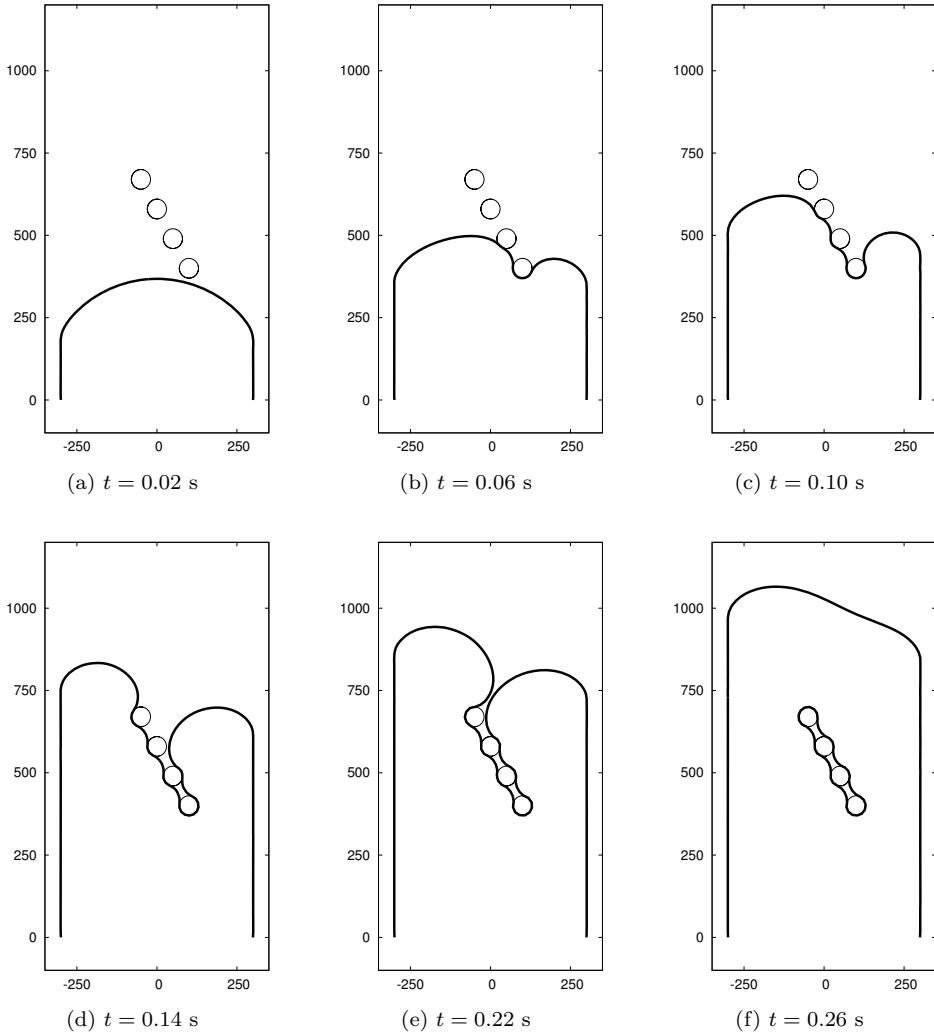


Fig. 5.2: Evolution through a cluster of obstacles and the formation of the Orowan island, $\tau_{app} = 40$ MPa, $t \in (0, 0.26)$, curve discretized by $M = 200$ nodes, dimensions in nm.

- [4] T. MURA. *Micromechanics of Defects in Solids*. Springer (1987)
- [5] M. BENEŠ, J. KRATOCHVÍL, J. KRÍŠŤAN, V. MINÁRIK, AND P. PAUŠ. *A Parametric Simulation Method for Discrete Dislocation Dynamics*. *European Physical Journal ST, Special Topics* **177** (2009) 177–192.
- [6] J. KRÍŠŤAN AND J. KRATOCHVÍL. *Interactions of glide dislocations in a channel of a persistent slip band*. *Philosophical Magazine* **87**, No. 29 (2007) 4593–4613.
- [7] J. KRÍŠŤAN, J. KRATOCHVÍL, V. MINÁRIK, AND M. BENEŠ. *Simulation of interacting dislocations glide in a channel of a persistent slip band*. *Modeling and Simulation in Materials Science and Engineering* **17** (2009), 045009
- [8] V. MINÁRIK, M. BENEŠ, AND J. KRATOCHVÍL. *Simulation of Dynamical Interaction between Dislocations and Dipolar Loops*. *J. Appl. Physics* **107** (2010), 061802.
- [9] V. MINÁRIK, J. KRATOCHVÍL. *Dislocation Dynamics – Analytical Description of the Interaction Force between Dipolar Loops*. *Kybernetika* **43** (2007), 841–854.

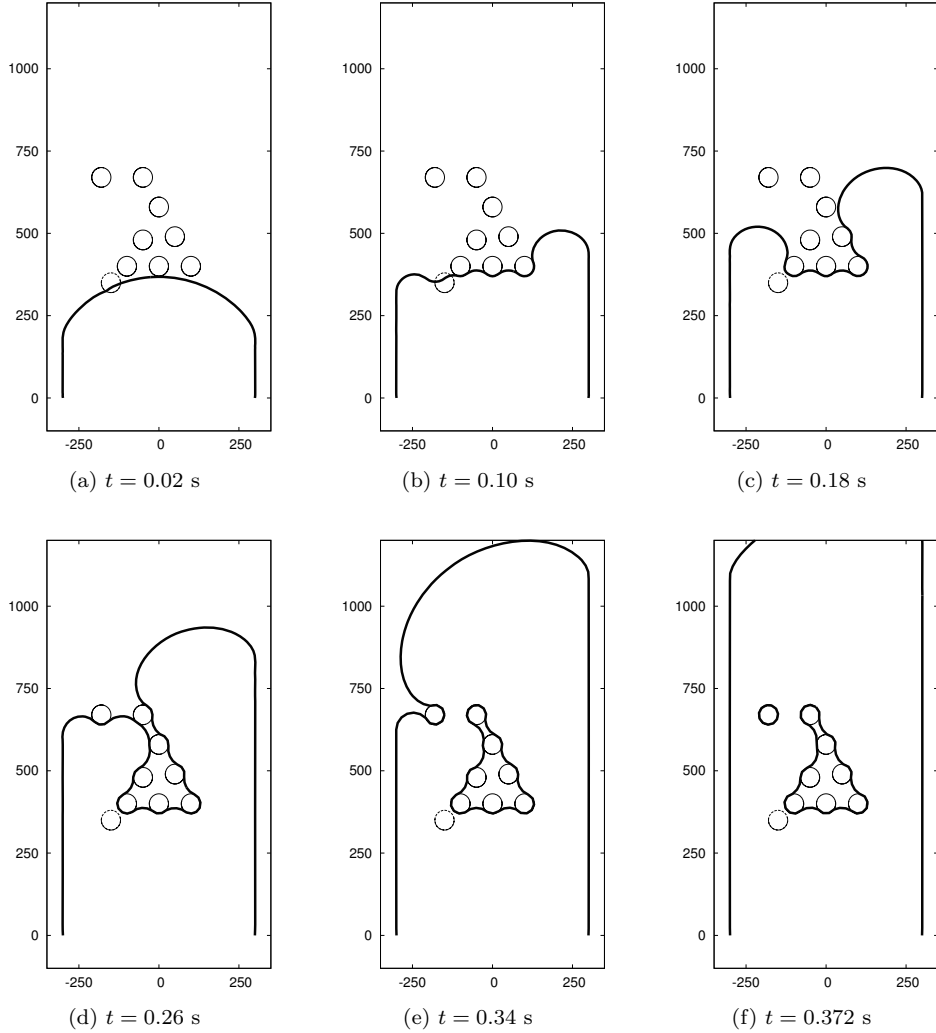


Fig. 5.3: Evolution through a random cluster of obstacles, weak obstacle and Orowan island, $\tau_{app} = 40$ MPa, $t \in (0, 0.26)$, curve discretized by $M = 200$ nodes, dimensions in nm.

- [10] V. MINÁRIK, J. KRATOCHVÍL AND K. MIKULA. *Numerical Simulation of Dislocation Dynamics by Means of Parametric Approach*. In: Beneš, M., Mikyška, J., Oberhuber, T. (eds.) Proceedings of the Czech Japanese Seminar in Applied Mathematics, Faculty of Nuclear Sciences and Physical Engineering, Czech Technical University in Prague, Prague, pp. 128–138 (2005).
- [11] V. MINÁRIK, J. KRATOCHVÍL, K. MIKULA AND M. BENEŠ. *Numerical simulation of dislocation dynamics*. In: Feistauer, M., Dolejší, V., Knobloch, P., Najzar, K. (eds.) Numerical Mathematics and Advanced Applications – ENUMATH 2003, Springer Verlag, New York, pp. 631–641 (2004).
- [12] P. PAUŠ. *Numerical simulation of dislocation dynamics*. In: M. Vajsáblová, P. Struk (eds.) Proceedings of Slovak-Austrian Congress, Magia, Bratislava, pp. 45–52 (2007).
- [13] P. PAUŠ, M. BENEŠ. *Algorithm for topological changes of parametrically described curves*. In: Handlovičová A., Frolkovič P., Mikula K., Ševčovič D. (eds.) Algorithmy 2009, Proceedings

- of contributed papers and posters Slovak University of Technology in Bratislava, Publishing House of STU, 2009, pp. 176–184 (2009).
- [14] P. PAUŠ, M. BENEŠ. *Direct approach to mean-curvature flow with topological changes*. Kybernetika **45** (2009), No. 4, 591–604.
 - [15] G. DZIUK, A. SCHMIDT, A. BRILLARD AND C. BANDLE. *Course on mean curvature flow*. Manuscript 75p., Freiburg (1994).
 - [16] J.A. SETHIAN. *Level set methods and fast marching methods*. Cambridge University Press, Cambridge (1999).
 - [17] S. OSHER AND R.P. FEDKIW. *Level set methods and dynamic implicit surfaces*. Springer, New York (2003).
 - [18] M. BENEŠ. *Phase field model of microstructure growth in solidification of pure substances*. Acta Math. Univ. Comenianae **70** (2001), 123–151.
 - [19] D. ŠEVČOVIČ AND S. YAZAKI. *On a motion of plane curves with a curvature adjusted tangential velocity*. In: <http://www.iam.fmph.uniba.sk/institute/sevcovic/papers/cl39.pdf>, arXiv:0711.2568, 2007.
 - [20] K. DECKELNICK AND G. DZIUK. *Mean curvature flow and related topics*. Frontiers in numerical analysis (2002) 63–108.
 - [21] E. OROWAN. *Dislocations in Metals*. AIME, New York, 1954
 - [22] L. M. BROWN. *The self-stress of dislocations and the shape of extended nodes*. Phil. Mag. **10** (1964).
 - [23] V. MOHLES. *Orowan process controlled dislocation glide in materials containing incoherent particles*. Materials Science and Engineering A **309310** (2001), 265–269.
 - [24] V. MOHLES. *Computer simulations of particle strengthening: lattice mismatch strengthening*. Materials Science and Engineering A **319321** (2001), 201–205.
 - [25] R. SEDLÁČEK. *Viscous glide of a curved dislocation*. Philosophical Magazine Letters **76**(4) (1997), 275–280.
 - [26] K. MIKULA AND D. ŠEVČOVIČ. *Evolution of plane curves driven by a nonlinear function of curvature and anisotropy*. SIAM J. Appl. Math. **61**, No. 5 (2001), 1473–1501.
 - [27] K. MIKULA, K. AND D. ŠEVČOVIČ. *Computational and qualitative aspects of evolution of curves driven by curvature and external force*. Computing and Visualization in Science **6**, No. 4 (2004), 211–225.